

Adsorbate-adsorbate interactions and chemisorption at different coverage studied by accurate *ab initio* calculations: CO on transition metal surfaces

Sara E. Mason, Ilya Grinberg and Andrew M. Rappe

The Makineni Theoretical Laboratories, Department of Chemistry

University of Pennsylvania, Philadelphia, PA 19104-6323

(Dated: August 27, 2018)

Abstract

We use density functional theory (DFT) with the generalized gradient approximation (GGA) and our first-principles extrapolation method for accurate chemisorption energies [Mason *et al.*, Phys. Rev. B **69**, 161401R (2004)] to calculate the chemisorption energy for CO on a variety of transition metal surfaces for various adsorbate densities and patterns. We identify adsorbate through-space repulsion, bonding competition, and substrate-mediated electron delocalization as key factors determining preferred chemisorption patterns for different metal surfaces and adsorbate coverages. We discuss how the balance of these interactions, along with the inherent adsorption site preference on each metal surface, can explain observed CO adsorbate patterns at different coverages.

I. INTRODUCTION

The prototypical CO/transition metal adsorption systems, though extensively studied, continue to be of significant contemporary research interest. [1, 2, 3] These systems owe their continued examination in part to the significant variations in CO bonding properties from one transition metal to another, such as the evolution of chemisorption geometry with adsorbate coverage Θ . Attempts to describe adsorption trends as a function of Θ are complicated by the many phenomena involved, such as through-space interactions between adsorbates, substrate-mediated interactions, surface relaxations and reconstructions induced by adsorption, adsorption at different high-symmetry sites, patterned overlayer formation, and transitions between different adsorbate arrangements on the surface under different conditions. [4, 5, 6, 7]

There are many studies that address adsorbate-adsorbate interactions [6, 8, 9, 10, 11, 12, 13, 14, 15], and it is beyond the present scope to review these and other studies in full. One major conclusion is that properties of sub-monolayer CO overlayers such as chemisorption energy and surface site occupation are found to be significantly coverage dependent. Interactions between CO molecules are strongly repulsive at short range; beyond nearest neighbor distance, inter-adsorbate interactions are non-monotonic and vary as a function of adsorbate coverage. A better understanding of adsorbate interactions would be helpful for understanding the wide variety of adsorption systems of interest to the surface science community. [11, 16, 17, 18, 19, 20]

To understand how chemisorption evolves with Θ , it is necessary to identify the factors influencing the adsorbate-adsorbate interactions, and how these factors vary from metal to metal. For this purpose, it is advantageous to have a data set spanning a variety of metals, and with a broad range (in terms of coverage, site occupancy, and overlayer pattern) of chemisorption geometries. With such a dataset, chemisorption energies between different CO overlayer structures can be compared for different metals, elucidating trends and revealing important interactions.

The goal of comparing chemisorption at different coverages, and at different adsorbate overlayer patterns for a given coverage, is well suited for theoretical study. We can model adsorption at coverages and in patterns not experimentally observed. However, it is necessary to have a means for accurately modeling chemisorption on a variety of metals, and

for all adsorption sites, coverages, and overlayers of interest. Owing to advances in computer power and algorithms, many aspects of surface science can be quantitatively explained through theoretical studies at the DFT-GGA level. [21, 22]

Hindering the use of DFT for quantitative investigation of CO/metal adsorption systems is the tendency of DFT calculations to overestimate chemisorption energies and to favor multiply coordinated adsorption sites over the top site, in disagreement with experimental data. This “CO/metal puzzle” was first comprehensively addressed by Feibelman *et al.*[23] Subsequently, several studies have traced the CO/metal puzzle to its origin. [24, 25, 26]

Following these investigations, we recently derived a first-principles extrapolation procedure [27] which, when applied to eight different single-crystal substrates, reduced overbinding and achieved site preferences consistent with experimentally observed adsorption in all cases. Other works discussing how to correct for the DFT site-preference problem include Olsen *et al.* [28] and Kresse *et al.* [26] In the work of Olsen *et al.*, relativistic effects are found to be important to correct site preferences for CO on Pt (111). However, this fails to explain why DFT finds incorrect site preference on non-relativistic Cu, as recently also pointed out by Gajdoš *et al.* [29] Kresse and co-workers employ a GGA+ U type exchange-correlation energy functional. However, the correct value of U is not known *a priori*. In contrast, our method uses *ab initio* calculations to unambiguously calculate the correction magnitude. The present work is the first time any of these three accurate methods has been applied to multiple metals, surfaces, and coverages in a single study.

II. METHODOLOGY AND COMPUTATIONAL DETAILS

In the present study, we investigate chemisorption of CO on transition metals as a function of metal, surface termination, adsorption site, and CO overlayer pattern. The focus of the present work is transition metal chemisorption, but some additional results for CO on Al (111) and (100) surfaces are also presented for the purpose of contrasting transition metals with an *sp* metal.

DFT calculations are carried out using the PBE GGA exchange-correlation functional [30] and norm-conserving optimized pseudopotentials [31] with the designed nonlocal method for metals. [32, 33] All pseudopotentials were designed using the OPIUM pseudopotential package. [34] Metal surfaces are modeled as $c(4 \times 2)$ or $p(2 \times 2)$ slabs of five layers separated

by vacuum, with atomic relaxation allowed in the two topmost layers. Calculations are done, and E_{chem} tested to be converged within less than 0.025 eV, using a $4 \times 4 \times 1$ grid of irreducible Monkhorst-Pack k -points. [35]

All values for E_{chem} reported here have been corrected using our first-principles extrapolation procedure. [27] We have tested that the corrections to E_{chem} do not appreciably evolve with Θ , affecting corrected values for E_{chem} by less than 0.01 eV/molecule. CO chemisorption is modeled at coverages of $\Theta=0.25$, $\Theta=0.5$, $\Theta=0.75$, and $\Theta=1$ ML (monolayer).

In these calculations, the CO bond is held perpendicular to the surface. Eliminating the CO tilt angle as a degree of freedom facilitates comparison of chemisorbed and gas-phase adsorbate-adsorbate interactions, as well as comparison of CO-CO interactions over different metals. None of the higher-coverage chemisorption structures on the (100) surfaces were found to have lateral forces on CO under this constraint. In some of the higher-coverage structures on the (111) surfaces, lateral forces of ≈ 0.01 – 0.05 eV/Å were found on the C and O atoms, as indicated in Table I. No dipole correction scheme to decouple the periodic slabs was included, as such corrections were found to affect the total energy of the chemisorption systems by less than 0.01 eV/cell.

Values for E_{chem} are calculated as

$$E_{\text{chem}} = (-E_{\text{surface-CO}} + NE_{\text{CO}} + E_{\text{surface}})/N \quad (1)$$

where N is the number of CO molecules per unit cell. With this definition, chemisorption energies are reported in eV/CO molecule, and positive values of E_{chem} represent favorable adsorption on the surface.

Note: The overlayer naming convention denotes both coverage and sites: one letter for $\Theta=0.25$, two for $\Theta=0.5$, three for $\Theta=0.75$, and four letters for $\Theta=1$.

On the (111) surfaces of Pt, Rh, and Pd, we modeled chemisorption at $\Theta=0.25$ at top (t), bridge (b), hcp (h) and fcc (f) adsorption sites, as shown in Figure 1(a). We consider our results for $\Theta=0.25$ to be the low-coverage limit values of E_{chem} . As a test of the validity of this assumption, we also calculated E_{chem} on each metal at each site in a $p(2 \times 3)$ cell, corresponding to a coverage of $\Theta=0.17$, on both the (111) and (100) surfaces. The change in E_{chem} from $\Theta=0.17$ to $\Theta=0.25$ was less than 0.04 eV for all sites and metals, with the same site preference. The most important characteristic of the t, b, f, and h arrangements is the absence of nearest neighbors.

At $\Theta=0.5$, we modeled chemisorption at top (tt) and hcp (hh) adsorption sites, as shown in Figure 1(b). We did not model fcc adsorption at $\Theta=0.5$ due to the very similar energies for f and h for all surfaces as shown in Table I. The tt and hh structures allow us to investigate how chemisorption changes when adsorbates are separated by nearest neighbor distances.

We model three different bridge site configurations, bb1, bb2, and bb3, as shown in Figures 1(b), 1(c), and 1(d). In bb1 and bb2, nearest neighbor CO molecules are present. For the bb2 configuration there is an additional characteristic: each surface metal atom involved in chemisorption participates in two carbon-metal bonds, leading to bonding competition. [4] The bb3 configuration does not have nearest neighbor CO molecules, and is one of the observed patterns at $\Theta=0.5$ on the Pd (111) surface. [36] Comparing these three bridge patterns allows us to deduce the energetic costs of nearest-neighbor adsorbate interactions and bonding competition for each metal.

We also considered (see Figure 2(a)) mixed occupation of top and bridge (tb) in a $c(4 \times 2)$ cell, the observed pattern at $\Theta=0.5$ on Pt (111) [37, 38, 39], and mixed occupation (see Figure 2(b)) of hcp and fcc (hf) in a $p(2 \times 2)$ cell, one of the observed patterns on Pd (111). [36] For the hf overlayer, bonding competition between CO molecules is present.

At $\Theta=0.75$, we modeled an overlayer with CO in top, hcp hollow, and fcc hollow (thf), Figure 2(b). This coverage and pattern is observed on both Rh and Pd (111) [36, 40, 41], and is another configuration where bonding competition is present.

Chemisorption at $\Theta=1$ is modeled in a $c(4 \times 2)$ cell for both top site (tttt) and hcp (hhhh) adsorption. Bonding competition cannot exist between top site adsorbed molecules, but is present in the hhhh configuration. Consistent with previous work, we find chemisorption at $\Theta=1$ to be exothermic. The lack of experimental observation of CO at $\Theta=1$ is due to kinetic effects. [42]

On the (100) surfaces of Pt, Rh, and Pd, we modeled chemisorption at $\Theta=0.25$ at top (t), bridge (b), and hollow (h) adsorption sites (see Figure 3(a)). As with the (111) surfaces, we consider adsorbates at this coverage to be isolated.

At $\Theta=0.5$ on (100) surfaces, we modeled chemisorption at two different top site configurations, tt1 and tt2, two different hollow site configurations, hh1 and hh2, and three different bridge site configurations, bb1, bb2, and bb3. These overlayer patterns are shown in Figures 3(b), 3(c), and 3(d). The top sites vary in that tt1 has CO molecules at nearest neighbor distances, while tt2 does not. Likewise, the hh1 overlayer has adsorbates at nearest

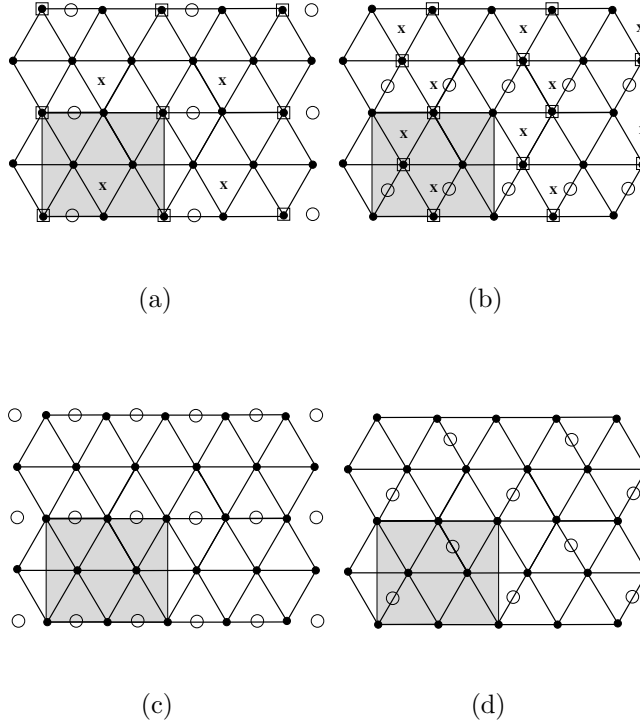


FIG. 1: (a) Schematic of (111) surfaces with CO at $\Theta=0.25$. Overlayer *t* is indicated by squares, *b* by circles, and *h* by "X". The cell is indicated by the shaded region. (b) Schematic of (111) surface with CO at $\Theta=0.5$ in overlayer *tt* (squares), in the *bb1* overlayer pattern (circles) and *hh* pattern ("X"). (c) Schematic of the (111) *bb2* structure. (d) Schematic of (111) *bb3* structure.

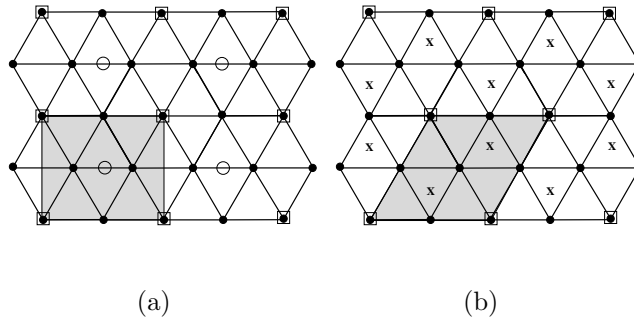


FIG. 2: (a) Schematic of (111) *tb* structure at $\Theta=0.5$. Occupied top sites are shown with squares, and occupied bridge sites are shown with circles. (b) Schematic of (111) *hf* and *thf* structures at $\Theta=0.5$ and $\Theta=0.75$. In the former, only hcp and fcc sites ("X") are occupied. In the latter, the top sites (squares) are also occupied.

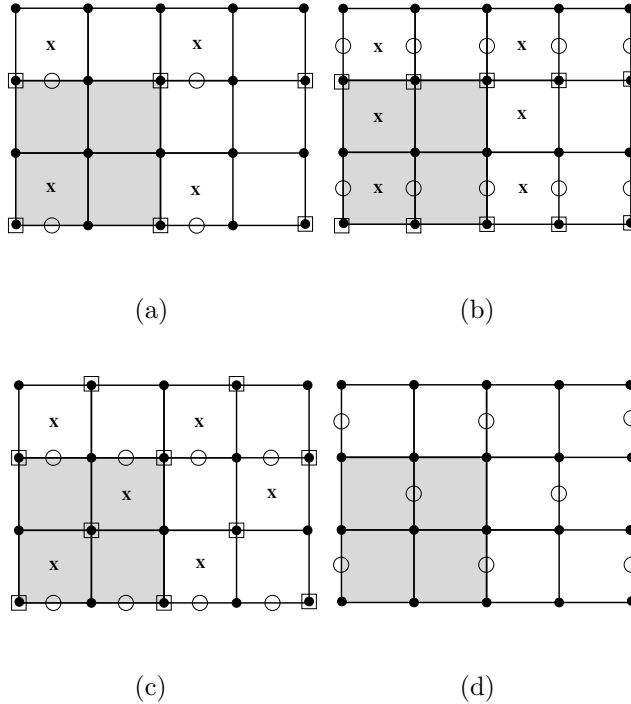


FIG. 3: (a) Schematic of (100) surface with CO at $\Theta=0.25$. Top site pattern t is indicated by squares, overlayer b by circles, and h by “X”. (b) Schematic of (100) $tt1$, $bb1$, and $hh1$ overlayers ($\Theta=0.5$). (c) Schematic of the (100) $tt2$, $bb2$, and $hh2$ overlayers. (d) Schematic of (100) $bb3$ structure with CO at $\Theta=0.5$.

neighbor separations while the $hh2$ overlayer does not. In the bridge site structures, both $bb1$ and $bb2$ have CO molecules at nearest neighbor separations, but differ in that $bb2$ has bonding competition while $bb1$ does not. The $bb3$ pattern is experimentally observed on both Pt and Rh (100). [43, 44] We also modeled $tttt$ and $hhhh$ adsorption at $\Theta=1$. All modeling of CO on the (100) surfaces was done in a $c(4 \times 2)$ cell.

III. RESULTS

We begin with low coverage ($\Theta=0.25$) results. Detailed comparison of these calculated energies and experimental results have been reported previously. [27] In the low-coverage limit, our calculations reproduce the site preferences observed experimentally for Rh, Pd and Pt (111) surfaces (top for Rh and Pt, fcc for Pd). [15] Experimental data show that the lowest-coverage ordered CO structure on all three of these (111) surfaces is $(\sqrt{3} \times$

$\sqrt{3})R30^\circ$ at $\Theta=0.33$. The formation of this overlayer is driven by nearest neighbor CO-CO repulsive interactions, since this overlayer gives the highest-coverage single-site occupation without nearest neighbor interactions. The site occupied in the $(\sqrt{3} \times \sqrt{3})R30^\circ$ structure is determined by the site preference of isolated CO adsorption.

The (100) surfaces of Pt, Rh, and Pd share common low-coverage chemisorption behavior. The lowest coverage at which ordered CO structures are observed on the (100) surfaces is $\Theta=0.5$. For (100) surfaces, we find that difference in E_{chem} between the $\Theta=0.25$ CO overlayer and the highest E_{chem} $\Theta=0.5$ CO overlayer is negligible, in agreement with experiments that find a $c(4 \times 2)$ overlayer at $\Theta=0.5$ to be the lowest coverage ordered structure. [15] On Pt (100), domains of top-site CO and of bridge-site CO are seen. [15] On Rh (100), CO occupies top sites at $\Theta=0.5$, and on Pd (100) CO binds at bridge sites. [15] For all three metals, our results for site preference at $\Theta=0.25$ are consistent with these experimental observations.

While Pd, Rh and Pt (111) surfaces form the same ordered structure at low coverage, they evolve differently with coverage. Comparison between DFT and experiment at higher Θ is imprecise due to our neglect of temperature, pressure, and entropy effects. However, our DFT results for $\Theta=0.5$ and 0 K are consistent with experimental results. Our calculations show that chemisorption of CO on Pt (111) at $\Theta=0.5$ in the $c(4 \times 2)$ tb mixed occupation structure is favored by ≈ 0.09 eV/molecule over the next highest E_{chem} overlayer, in agreement with the experimental observations of the $c(4 \times 2)$ tb structure at $\Theta=0.5$. [37, 38, 39] For Pd (111) we find that the bb3 $c(4 \times 2)$ structure is favored by ≈ 0.04 eV over the $c(4 \times 2)$ hf structure. All other overlayer patterns show E_{chem} values more than 0.1 eV lower than the hf and bb3 structures. This result is in agreement with coexistence of $c(4 \times 2)$ bb3 and hf overlayers at $\Theta=0.5$ observed on Pd (111) in low-temperature STM experiments. [36]

The case of Rh (111) is especially interesting, with the experimental LEED pattern showing disorder at $\Theta=0.5$. [40, 41] Our results show that the bb3, tb, and hf overlayers on Rh (111) at $\Theta=0.5$ have the same E_{chem} to within 0.03 eV. The experimental result may be due to full disorder, but our computations lead us to suggest that domains of several nearly isoenergetic overlayer patterns coexist, explaining the complicated LEED pattern.

For Pt (100) and Rh (100) surfaces, we find a small energy difference between the top and bridge site, consistent with the occupation of both of these sites for $\Theta=0.5$ and greater. [43, 44] For Pd (100), the large site preference energy is consistent with experimental observation

TABLE I: Results for CO E_{chem} at different Θ on the (111) surfaces of Pt, Rh, and Pd, in eV. Selected Al values are also reported. For coverages above $\Theta=0.25$, the difference E_{int} between the low-coverage value and high-coverage value E_{chem} for the corresponding sites is reported in parenthesis. Values for experimentally observed structures are in italics. * indicates systems for which the lateral forces on CO were not minimized (CO is constrained to be perpendicular in all cases).

	Pt (111)		Rh (111)		Pd (111)		Al (111)	
	E_{chem}	E_{int}	E_{chem}	E_{int}	E_{chem}	E_{int}	E_{chem}	E_{int}
$\Theta=0.25$								
t	1.56		1.67		1.25		0.22	
b	1.43		1.58		1.49			
h	1.40		1.64		1.60			
f	1.43		1.64		1.63			
$\Theta=0.5$								
tt	1.27	0.29	1.35	0.32	0.93	0.32	0.17	0.05
bb1*	1.12	0.31	1.25	0.33	1.15	0.34		
bb2	1.07	0.36	1.40	0.18	1.09	0.40		
bb3*	1.36	0.07	1.55	0.03	1.44	0.05		
tb*	1.45	0.04	1.56	0.06	1.31	0.06		
hh*	1.03	0.37	1.33	0.31	1.19	0.41		
hf	1.21	0.20	1.53	0.11	1.40	0.21		
$\Theta=0.75$								
thf*	1.19	0.27	1.39	0.26	1.15	0.34		
$\Theta=1$								
tttt	0.74	0.82	0.53	1.14	0.39	0.86		
hhhh*	0.31	1.09	0.76	0.88	0.46	1.14		

that only bridge sites are occupied for all values of Θ . [45]

TABLE II: Same as Table I, for CO chemisorption on (100) surfaces.

	Pt (100)		Rh (100)		Pd (100)		Al (100)	
	E_{chem}	E_{int}	E_{chem}	E_{int}	E_{chem}	E_{int}	E_{chem}	E_{int}
$\Theta=0.25$								
t	1.80		1.72		1.35		0.12	
b	1.83		1.77		1.64			
h	1.25		1.60		1.50			
$\Theta=0.5$								
tt1	1.49	0.31	1.39	0.33	1.01	0.34	0.07	0.05
tt2	1.78	0.02	1.72	0.00	1.34	0.01		
bb1	1.60	0.23	1.47	0.30	1.36	0.28		
bb2	1.50	0.33	1.58	0.19	1.28	0.36		
bb3	1.77	0.06	1.73	0.04	1.62	0.02		
hh1	0.83	0.42	1.23	0.37	1.10	0.40		
hh2	1.08	0.17	1.49	0.11	1.35	0.15		
$\Theta=1$								
tttt	1.16	0.64	1.08	0.64	0.70	0.65		
hhhh	0.11	1.14	0.73	0.87	0.38	1.12		

IV. DISCUSSION

In this section, we discuss trends in the data presented in Tables I and II. We identify the presence of nearest neighbors and/or metal-atom sharing as the chief determinants of interactions between adsorbed CO molecules.

The effects of the substrate on adsorbate-adsorbate interactions will be discussed in the framework of the Hammer-Morikawa-Nørskov model [46] for the d -band contribution to top-site CO chemisorption:

$$\begin{aligned}
 E_{\text{chem}}^d = & 4 \left[\frac{fV_{\pi}^2}{(\epsilon_{2\pi^*} - \epsilon_d)} + fS_{\pi}V_{\pi} \right] \\
 +2 & \left[(1-f) \frac{V_{\sigma}^2}{(\epsilon_d - \epsilon_{5\sigma})} + (1+f)S_{\sigma}V_{\sigma} \right]
 \end{aligned} \tag{2}$$

where f is the idealized filling of the metal d bands, V_{π}^2 is the metal-carbon orbital overlap matrix element at the top site, $\epsilon_{2\pi^*}$ and $\epsilon_{5\sigma}$ are the energies of the renormalized $2\pi^*$ and 5σ orbitals relative to the Fermi level, and ϵ_d is the center of the metal d -bands relative to the Fermi level. V and S are coupling and overlap matrix elements respectively, and are labeled by orbital.

We also analyze gas-phase CO-CO interactions, study induced charge densities in chemisorbed systems, and analyze the metal electronic structure.

A. Nearest-neighbor interactions and chemisorption-induced perturbations

We now analyze the E_{chem} results presented in Section III to understand nearest-neighbor adsorbate-adsorbate interactions, for systems that have no metal-atom sharing.

We can estimate the energetic cost of placing adsorbates at nearest neighbor distances from our top-site chemisorption results. Our dataset includes three different exclusively top site chemisorbed structures at $\Theta=0.5$: The tt structure on (111) (see Figure 1(b)), and the tt1 and tt2 structures on the (100) surface (see Figures 3(b) and 3(c)). While the chemisorbed CO molecules in the tt and tt1 structures have nearest-neighbor CO adsorbates, the adsorbates in the tt2 structure do not. From inspection of the data in Tables I and II, it is clear that E_{int} (the difference between the low-coverage limit and higher coverage E_{chem}) for the tt2 structure on the (100) surface is tiny (≤ 0.02 eV) for all metals. E_{int} is much larger but still nearly independent of metal identity for the tt and tt1 patterns ($= 0.32 \text{ eV} \pm 0.02 \text{ eV}$). E_{int} for the Al surfaces is almost an order of magnitude smaller than for the transition metal surfaces.

We can compare these E_{int} results with the gas-phase CO-CO interaction energy $E_{\text{int}}^{\text{gas}}$, calculated by:

$$E_{\text{int}}^{\text{gas}}(r) = E_{\text{CO-CO}}^{\text{gas}} - 2E_{\text{CO}} \quad (3)$$

The interaction energy for CO at different separations is plotted in Figure 4. At the nearest-neighbor separations for Al (2.89 Å), Pt (2.76 Å), Pd (2.73 Å), and Rh (2.66 Å), the gas-phase CO-CO interaction energies are 0.12, 0.19, 0.21, and 0.27 eV, respectively. The

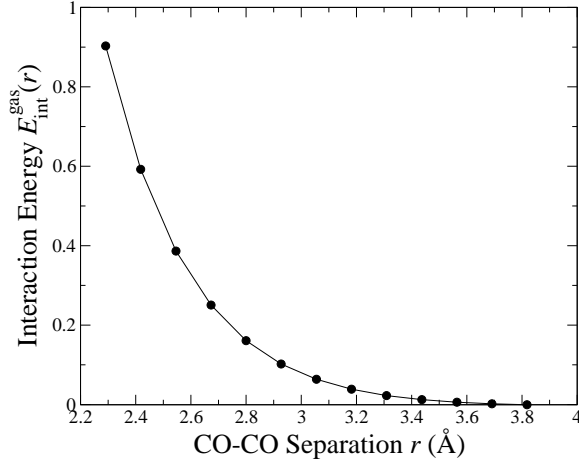


FIG. 4: Calculated interaction energy $E_{\text{int}}^{\text{gas}}(r)$ for 2 CO molecules at different separations r .

corresponding (111) tt E_{int} values from Table I are 0.05, 0.30, 0.32, and 0.32 eV, respectively. For Al, $E_{\text{int}} < E_{\text{int}}^{\text{gas}}$, suggesting that the s and p metal electrons do not increase CO-CO repulsion and perhaps lessen it somewhat. The transition metals all show $E_{\text{int}} > E_{\text{int}}^{\text{gas}}$, meaning that through-space repulsion is augmented by the surface. From the contrast with Al, we deduce that this increase in repulsion must be due to d electrons changing the adsorbed CO electronic structure.

The Hammer-Morikawa-Nørskov model (Equation 2) shows that the back-donation from the metal d -bands into the CO $2\pi^*$ increases with f . Increased filling of the $2\pi^*$ orbitals strengthens the repulsion between chemisorbed CO molecules, while increased inter-adsorbate separation weakens it. Pt and Pd have a higher f but a greater CO-CO separation than on Rh. Our data indicate that these effects balance, giving nearly the same CO-CO interaction energy (top-site E_{int}) for these three transition metals.

The bridge-site systems show the same E_{int} trends. For systems with no first nearest neighbors (bb3) E_{int} is very small. For bridge overlayers at $\Theta=0.5$ with nearest neighbors but no metal-atom sharing (bb1), a large metal-independent $E_{\text{int}} \approx 0.32$ eV is observed, just as for top sites. (Actually, the bb1 pattern on Pt (100) is somewhat more stable; this surface is known to reconstruct, so chemisorption may be stabilized by relieving surface stress. [43, 47, 48, 49] The changes in E_{chem} we do observe on the unreconstructed Pt(100) surface are in excellent agreement with other recent theoretical work. [3])

Nearest-neighbor hollow sites always involve metal atom sharing, so they are considered in the next section.

TABLE III: Values for the d -band center, ϵ_d , for the (111) and (100) surfaces of Pt, Rh, and Pd when no CO is adsorbed ($\Theta=0$), and when CO is adsorbed at bridge site at $\Theta=0.25$. The changes in ϵ_d due to chemisorption (Δ) are also listed. All reported values are in eV.

	$\Theta=0$	$\Theta=0.25$	Δ
Pt (111)	-2.93	-3.59	-0.66
Pt (100)	-2.79	-3.50	-0.71
Pd (111)	-2.29	-3.04	-0.75
Pd (100)	-2.17	-2.94	-0.77
Rh (111)	-2.42	-2.85	-0.43
Rh (100)	-2.29	-2.73	-0.44

B. Metal-atom sharing: bonding competition and electron delocalization

Bonding competition arises when the surface metal atoms involved in chemisorption participate in more than one carbon-metal bond. To find the susceptibility of E_{chem} to external perturbation (such as the sharing of metal atoms) within the Hammer-Morikawa-Nørskov model, we differentiate the expression for E_{chem}^d (Equation 2) with respect to external parameter λ , representing the number of chemisorption bonds per metal atom:

$$\frac{dE_{\text{chem}}^d}{d\lambda} = \left[\frac{4fV_{\pi}^2}{(\epsilon_{2\pi^*} - \epsilon_d)^2} - \frac{2(1-f)V_{\sigma}^2}{(\epsilon_d - \epsilon_{5\sigma})^2} \right] \frac{d\epsilon_d}{d\lambda} \quad (4)$$

The opposite signs of the two terms in Equation 4 mean that any change in the position of ϵ_d has two competing effects on E_{chem} . This competition vanishes as $f \rightarrow 1$, so E_{chem} on Pd or Pt ($f=0.9$) should be more sensitive to bonding competition than Rh ($f=0.8$).

The change of E_{chem} with bonding competition λ also depends on $d\epsilon_d/d\lambda$, the shift in the d -band energy as chemisorption bonds are formed. The ϵ_d position is affected by perturbation to the metal surface such as strain [50, 51], alloying [46, 52] and creation of chemical bonds with adsorbates. [4, 53] This effect is explored in Table III, showing that CO chemisorption causes a much smaller shift in ϵ_d for Rh than for either Pd or Pt.

The preceding analysis of the Hammer-Morikawa-Nørskov model suggests that bonding competition should increase E_{int} for all chemisorption involving metal sharing, but much less on Rh than on Pt or Pd, due to lower f and lower $d\epsilon_d/d\lambda$.

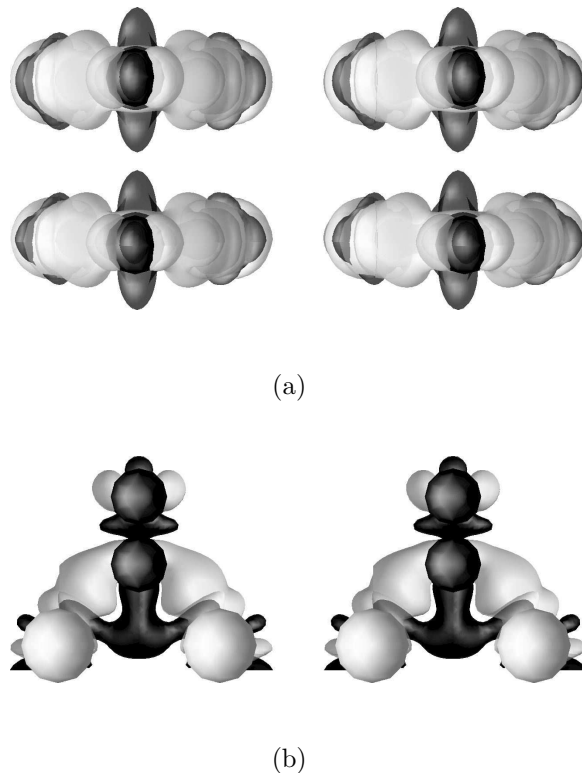


FIG. 5: Charge density changes induced by CO adsorption in pattern bb1 site on Pt (100). Lightly shaded iso-surfaces show areas of charge gain, and darker iso-surfaces show areas of charge loss. (a) Top view. (b) Side view.

In addition to the destabilizing effect of bonding competition, metal-atom sharing also enables electron delocalization. As illustrated in Figures 5 and 6, the CO $2\pi^*$ orbitals of neighboring molecules and the metal d orbitals of the atom they share combine to form extended states in the bb2 system (Figure 6). This delocalization is not present on the bb1 overlayer (Figure 5).

For the bridge-bonded systems with metal-atom sharing (bb2), the effect is dramatic. On Rh (111) and (100), delocalization stabilizes chemisorption significantly, and bonding competition gives a only small reduction, leading to stronger chemisorption and E_{int} values that are 0.1–0.15 eV lower for bb2 than for bb1. On Pt and Pd, much stronger bonding competition destabilizes chemisorption, raising E_{int} for bb2 about 0.15–0.2 eV above that of Rh, and 0.05–0.1 eV above the bb1 values on Pt and Pd despite electron delocalization.

Hollow site chemisorption exhibits the same trends, with bonding competition making bonding less effective, and metal-mediated delocalization stabilizing metal-sharing

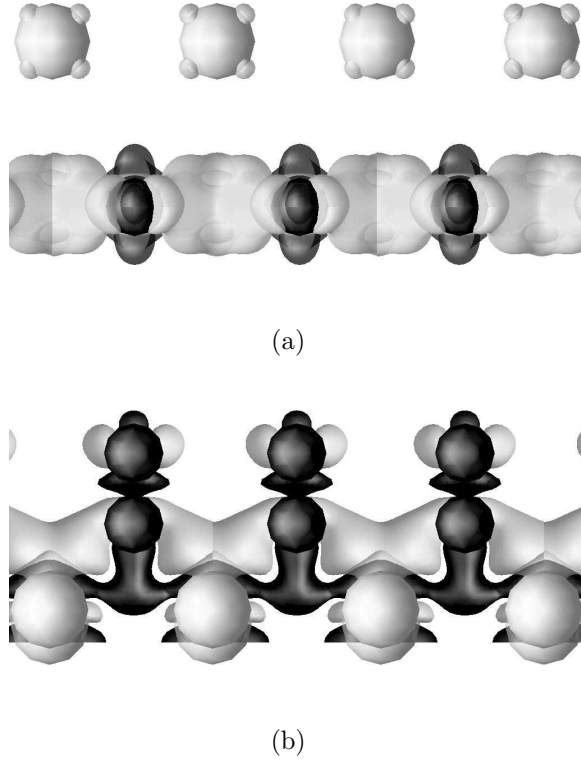


FIG. 6: Same as Figure 5, for the bb2 overlayer. Note the significant charge sharing between neighboring CO molecules, mediated by the shared metal atom.

chemisorption. However, because a CO at a hollow site distributes its bonding among three or four surface atoms, both the bonding competition and delocalization effects from metal sharing are somewhat less than for bridge sites. In all cases (hh, hh1, hh2) E_{int} for Rh is more favorable by ≈ 0.05 eV than on Pt and Pd. Since E_{int} at hh and hh1 is greater than at tt and tt1, metal sharing appears to always be net repulsive for hollow sites.

C. Preferred Overlayer Structures

In this section we discuss how adsorbate-adsorbate interactions, along with the low-coverage CO site preference on each surface, influence E_{chem} for various $\Theta=0.5$ overlayers.

On the (111) surfaces of Pt, Pd, and Rh, we modeled chemisorption at $\Theta=0.5$ for seven different overlayer patterns. In the case of Pt (111), we find tb (experimentally observed on Pt (111) [37, 38, 39]) has the highest E_{chem} , by at least 0.09 eV over the other overlayer patterns. At low coverage, t is preferred by 0.13 eV over b and f, and by 0.16 eV over h.

On the (111) surface, exclusive occupation of top sites (at $\Theta \geq 0.5$) must involve nearest-neighbor adsorbates, whereas the mixed occupation tb avoids nearest neighbors, reducing through-space repulsion. Therefore, the tb structure can be viewed as a compromise between the site preference for t, and reduced adsorbate-adsorbate repulsion made possible by partial b occupation.

On Pd (111), we find E_{chem} for bb3 and hf (both of which are experimentally observed [36]) to be within 0.04 eV of each other, and at least 0.09 eV stronger than the other five patterns. At low coverage, we find f to be preferred by 0.14 eV over b. Here we can also interpret the hf and bb3 overlayer patterns to be compromises between inherent site preference and adsorbate-adsorbate repulsion minimization. In the bb3 pattern, the occupation of less-favored bridge sites is compensated by reduced adsorbate-adsorbate through-space repulsion and absence of metal sharing. Conversely, occupying the preferred hollow sites in the hf arrangements comes at the expense of metal sharing, which we have discussed as being unfavorable for Pd.

On Rh (111) we find bb3, tb, and hf overlayer patterns to have the same E_{chem} within 0.03 eV. At low coverage, we find that Rh has a relatively weak inherent site preference, preferring t over b by 0.09 eV, and t over h and f by only 0.03 eV. Since both site preference and repulsion due to metal sharing are weak on Rh, we can explain the stronger E_{chem} of bb3, tb, and hf as being due to not having any nearest-neighbor CO distances. The other four overlayers studied all have some nearest neighbors.

On the (100) surfaces of Pt, Pd, and Rh, mixed site occupation is not observed at $\Theta=0.5$. The square lattice geometry of the (100) surface permits single-site occupancy at $\Theta=0.5$ without nearest neighbors. As a result (contrary to the (111) surface), a tb arrangement on the (100) surface would introduce adsorbates at shorter separations than in the tt2 arrangement. Therefore, on (100) surfaces we would expect overlayer patterns that minimize through-space repulsion and free of bonding competition most likely to be observed. Both tt2 and bb3 minimize adsorbate-adsorbate through-space repulsions and do not involve bonding competition, and this explains why we find E_{int} to be no greater than 0.06 eV for these patterns on all three metals.

V. CONCLUSION

We have presented for the first time results for CO chemisorption at different coverages using DFT-GGA plus our first-principles extrapolation procedure for accurate chemisorption energies. Our values for E_{chem} at higher coverage with CO occupying different sites and in different patterns show the experimentally observed structure to have the most favorable E_{chem} within the selection of adsorbate arrangements modeled. We identify and discuss adsorbate through-space repulsion, bonding competition, and substrate-mediated electron delocalization as key factors determining preferred chemisorption patterns for different metal surfaces and adsorbate coverages. We rationalize how these effects, along with the inherent site preference energy for CO on each metal, balance to cause different trends in chemisorption behavior as a function of CO coverage Θ on different transition metal surfaces.

VI. ACKNOWLEDGMENTS

This work was supported by the Air Force Office of Scientific Research, Air Force Materiel Command, USAF, under grant number FA9550-04-1-0077, and the NSF MRSEC Program, under Grant DMR05-20020. Computational support was provided by the Defense University Research Instrumentation Program, the High Performance Computing Modernization Office of the Department of Defense, and by the National Science Foundation CRIF Program, Grant CHE-0131132. SEM thanks Alexie M. Kolpak and Valentino R. Cooper for testing and discussions of dipole corrections to chemisorption system energies.

-
- [1] N. A. Besley, *J. Chem. Phys.* **122**, 1847006 (2005).
 - [2] T. Mitsui, M. K. Rose, E. Fomin, D. F. Ogletree, and M. Salmeron, *Phys. Rev. Lett.* **94**, 0336101 (2005).
 - [3] S. Yamagishi, T. Fujimoto, Y. Inada, and H. Orita, *J. Phys. Chem. B* **109**, 8899 (2005).
 - [4] B. Hammer, *Phys. Rev. B* **63**, 205423 (2001).
 - [5] R. Linke, D. Curulla, M. J. P. Hopstaken, and J. W. Niemantsverdriet, *J. Chem. Phys.* **115**, 8209 (2001).
 - [6] B. N. J. Persson, M. Tüshaus, and A. M. Bradshaw, *J. Chem. Phys.* **92**, 5034 (1990).

- [7] A. B. Gurney, L. J. Richter, J. S. Villarrubia, and W. Ho, *J. Chem. Phys.* **87**, 6710 (1987).
- [8] R. Brako and D. Šokčević, *Surf. Sci.* **469**, 185 (2000).
- [9] A. P. van Bavel, M. J. P. Hopstaken, D. Curulla, J. W. Niemantsverdriet, J. J. Lukkien, and P. A. J. Hilbers, *J. Chem. Phys.* **119**, 524 (2003).
- [10] H. S. Kato, H. Okuyama, J. Yoshinobu, and M. Kawai, *Surf. Sci.* **513**, 239 (2002).
- [11] F. Zaera, *J. Phys. Chem. B* **106**, 4043 (2002).
- [12] R. Kose, W. A. Brown, and D. A. King, *J. Phys. Chem. B* **103**, 8722 (1999).
- [13] L. Österlund, M. Ø. Pedersen, I. Stensgaard, E. Lægsgaard, and F. Besenbacher, *Phys. Rev. Lett.* **83**, 4812 (1999).
- [14] S. D. Kevan, *J. Mol. Catal. A: Chem.* **131**, 19 (1998).
- [15] D. H. Wei, D. C. Skelton, and S. D. Kevan, *Surf. Sci.* **381**, 49 (1997).
- [16] Q. Ge, , and M. Neurock, *J. Am. Chem. Soc.* **2004**, 1551 (2003).
- [17] Z.-P. Liu and P. Hu, *J. Am. Chem. Soc.* **125**, 1958 (2003).
- [18] W. Mar and M. L. Klein, *Langmuir* **10**, 188 (1994).
- [19] M. Tarek, K. Tu, M. L. Klein, and D. J. Tobias, *Biophysical J.* **77**, 964 (1999).
- [20] Y. Yourdshahyan, H. Zhang, and A. M. Rappe, *Phys. Rev. B Rapid Comm.* **63**, 081405(R) (2001).
- [21] A. Groß, *Theoretical Surface Science* (Springer, 2003).
- [22] J. Greeley, J. Nørskov, and M. Mavrikakis, *Annu. Rev. Phys. Chem.* **53**, 319 (2002).
- [23] P. J. Feibelman, B. Hammer, J. K. Nørskov, F. Wagner, M. Scheffler, R. Stumpf, R. Watwe, and J. Dumesic, *J. Phys. Chem. B* **105**, 4018 (2001).
- [24] I. Grinberg, Y. Yourdshahyan, and A. M. Rappe, *J. Chem. Phys.* **117**, 2264 (2002).
- [25] A. Gil, A. Clotet, J. M. Ricart, G. Kresse, M. Garcia-Hernandez, N. Rosch, and P. Sautet, *Surf. Sci.* **530**, 71 (2003).
- [26] G. Kresse, A. Gil, and P. Sautet, *Phys. Rev. B* **68**, 073401 (2003).
- [27] S. E. Mason, I. Grinberg, and A. M. Rappe, *Phys. Rev. B Rapid Comm.* **69**, 161401(R) (2004).
- [28] R. A. Olsen, P. H. T. Philipsen, and E. J. Baerends, *J. Chem. Phys.* **119**, 4522 (2003).
- [29] M. Gajdoš and J. Hafner, *Surf. Sci.* **590**, 117 (2005).
- [30] J. P. Perdew, K. Burke, and M. Ernzerhof, *Phys. Rev. Lett.* **77**, 3865 (1996).
- [31] A. M. Rappe, K. M. Rabe, E. Kaxiras, and J. D. Joannopoulos, *Phys. Rev. B Rapid Comm.* **41**, 1227 (1990).

- [32] N. J. Ramer and A. M. Rappe, *Phys. Rev. B* **59**, 12471 (1999).
- [33] I. Grinberg, N. J. Ramer, and A. M. Rappe, *Phys. Rev. B Rapid Comm.* **63**, 201102(R) (2001).
- [34] <http://opium.sourceforge.net>.
- [35] H. J. Monkhorst and J. D. Pack, *Phys. Rev. B* **13**, 5188 (1976).
- [36] M. K. Rose, T. Mitsui, J. Dunphy, A. Borg, D. F. Ogletree, M. Salmeron, and P. Sautet, *Surf. Sci.* **512**, 48 (2002).
- [37] M. Ø. Pederson, M. L. Bocquet, P. Sautet, E. Lægsgaard, I. Stensgaard, and F. Besenbacher, *Chem. Phys. Lett.* **299**, 403 (1999).
- [38] D. F. Ogletree, M. A. Vanhove, and G. A. Somorjai, *Surf. Sci.* **173**, 351 (1986).
- [39] F. Bondino, G. Comelli, F. Esch, A. Locatelli, A. Baraldi, S. Lizzit, G. Paolucci, and R. Rosei, *Surf. Sci.* **459**, L467 (2000).
- [40] A. Beutler, E. Lundgren, R. Nyholm, J. N. Andersen, B. J. Setlik, and D. Heskett, *Surf. Sci.* **396**, 117 (1998).
- [41] A. Beutler, E. Lundgren, R. Nyholm, J. N. Andersen, B. J. Setlik, and D. Heskett, *Surf. Sci.* **381**, 381 (1997).
- [42] J. A. Steckel, A. Eichler, and J. Hafner, *Phys. Rev. B* **68**, 085416 (2003).
- [43] R. Martin, P. Gardner, and A. M. Bradshaw, *Surf. Sci.* **342**, 69 (1995).
- [44] A. Baraldi, L. Gregoratti, G. Comelli, V. R. Dhanak, M. Kiskinova, and R. Rosei, *Appl. Surf. Sci.* **99**, 1 (1996).
- [45] A. M. Bradshaw and F. M. Hoffmann, *Surf. Sci.* **72**, 513 (1978).
- [46] B. Hammer, Y. Morikawa, and J. K. Nørskov, *Phys. Rev. Lett.* **76**, 2141 (1996).
- [47] W. A. Brown, R. Kose, and D. A. King, *Chem. Rev.* **98**, 797 (1998).
- [48] A. E. Morgan and G. A. Somorjai, *Surf. Sci.* **12**, 405 (1968).
- [49] A. E. Morgan and G. A. Somorjai, *J. Chem. Phys.* **51**, 3309 (1969).
- [50] M. Mavrikakis, B. Hammer, and J. K. Nørskov, *Phys. Rev. Lett.* **81**, 2819 (1998).
- [51] M. W. Wu and H. Metiu, *J. Chem. Phys.* **113**, 1177 (2000).
- [52] J. Greeley and M. Mavrikakis, *Nature Materials* **3**, 810 (2004).
- [53] A. Ruban, B. Hammer, P. Stoltze, H. L. Skriver, and J. K. Nørskov, *J. Mol. Catal. A: Chem.* **115**, 421 (1997).